

PAPER • OPEN ACCESS

## Flow-enhanced remelting of settling/floating globular crystals during mixed columnar-equiaxed solidification

To cite this article: M Wu *et al* 2023 *IOP Conf. Ser.: Mater. Sci. Eng.* **1281** 012036

View the [article online](#) for updates and enhancements.

### You may also like

- [Effects of Yttrium on the pitting corrosion behavior of 304 stainless steel with coating by laser remelting](#)  
Mengnan Liu, Dongxu Chen, Yanan Wang et al.
- [Incorporation of fragmentation into a volume average solidification model](#)  
Y Zheng, M Wu, A Kharicha et al.
- [Effect of surface modification through GTAW on high-temperature performance of 4Cr5MoSiV steel](#)  
Yangchuan Cai, Yan Cui, Lisong Zhu et al.



**HONOLULU, HI**  
Oct 6–11, 2024

Abstract submission deadline:  
**April 12, 2024**

**Learn more and submit!**



**Joint Meeting of**

The Electrochemical Society  
•  
The Electrochemical Society of Japan  
•  
Korea Electrochemical Society

# Flow-enhanced remelting of settling/floating globular crystals during mixed columnar-equiaxed solidification

M Wu\*, Z Zhang, H Zhang, A Ludwig, A Kharicha

Chair for Simulation and Modeling of Metallurgy Processes, Department of Metallurgy, University of Leoben, A-8700 Leoben, Austria

E-mail: menghuai.wu@unileoben.ac.at

**Abstract.** Previously, the authors have used a mixed columnar-equiaxed solidification model, successfully ‘reproduced’ the solidification benchmark experiments on the Sn-10wt.%Pb alloy under natural/forced convections (travelling magnetic stirring) as performed at SIMAP laboratory [*Int. J. Heat Mass Transf.* **85** (2015) 438-54]. The current contribution is to address the flow-effect on the remelting of settling/floating crystals during the mixed columnar-equiaxed solidification. The remelting or growth is controlled by diffusion of solute in the liquid boundary layer. The diffusion length due to the flow-effect is modelled as a function of Schmidt and Reynolds numbers. The modelling results show that remelting rate of the floating/settling crystals, which originate from fragmentation and then brought to the superheated region by the forced flow, can be enhanced by the flow. In turn the released latent heat can reduce the temperature locally (even globally), hence to speed up the solidification of the columnar structure. Additionally, the solidification-migration-remelting of equiaxed grains present an important macrosegregation mechanism. By solidification of a crystal in the cold region it rejects solute, while by remelting of the crystal it dilutes the surrounding melt. These phenomena are found critical in many engineering castings with mixed columnar-equiaxed solidification.

## 1. Introduction

Solidification and remelting occur concurrently during solidification of many engineering castings. As shown in figure 1(a), a crystal with certain  $mass$ , which forms near the mold wall, would release the latent heat  $mass \cdot L$  and reject solute  $mass \cdot c_\ell^* \cdot (1-k)$  in its surrounding melt. When this crystal is transported to a superheat region and re-melted there, it would take the same amount of energy  $-mass \cdot L$  from melt of its new surrounding and dilute the melt there  $-mass \cdot c_\ell^* \cdot (1-k)$ . This concurrent solidification-remelting phenomenon, together with grain transport, is critical for a numerical model [1]. This conference contribution is (1) to quantify the importance of the remelting effect in the alloy solidification and (2) to address the flow-effect on the remelting. As shown in figure 1(b) and (c), the solidification/remelting rate, i.e. the formed or re-melted  $mass$  is proportional to growth or shrinkage velocity of the crystal  $v_R$ , with + or - sign of its value indicating the growth or shrinkage of the radius of the globular grain.

$$v_R = \frac{D_\ell}{l_\ell} \cdot \frac{(c_\ell^* - c_\ell)}{(c_\ell^* - c_\ell^{\text{interface}})}, \quad (1)$$

where  $D_\ell$  is the diffusion coefficient of solute in the melt.  $c_\ell$  and  $c_\ell^*$  are bulk and thermodynamic equilibrium concentrations.  $c_\ell^{\text{interface}}$  is the so-called interface concentration at the crystal surface, which is assumed as the



equilibrium concentration of the crystal  $c_e^*$  for solidification and the average concentration of the crystal  $c_e$  for remelting. Here we ignore the back diffusion in the solid crystal. The flow effect is described by the adapted diffusion length in the liquid boundary layer  $l_\ell$ , which is a function of the Reynolds and Schmidt numbers. For solidification [2],

$$l_\ell = \min \left( \frac{D_\ell}{v_R}, R \left[ \frac{1}{1-f_e^{1/3}} + \frac{Sc^{1/3} Re^n}{3f_\ell} \right]^{-1} \right), \quad (2)$$

for remelting [3],

$$l_\ell = \frac{R}{1.0 + 0.3 \cdot Sc^{1/3} Re^{1/2}}, \quad (3)$$

where  $n = \frac{1}{3} + \frac{Re^{0.28}}{3(Re^{0.28} + 4.65)}$ ,  $Re = \frac{d_e \rho_\ell |\vec{u}_\ell - \vec{u}_e|}{\mu}$  and  $Sc = \frac{\mu}{\rho_\ell D_\ell}$ .

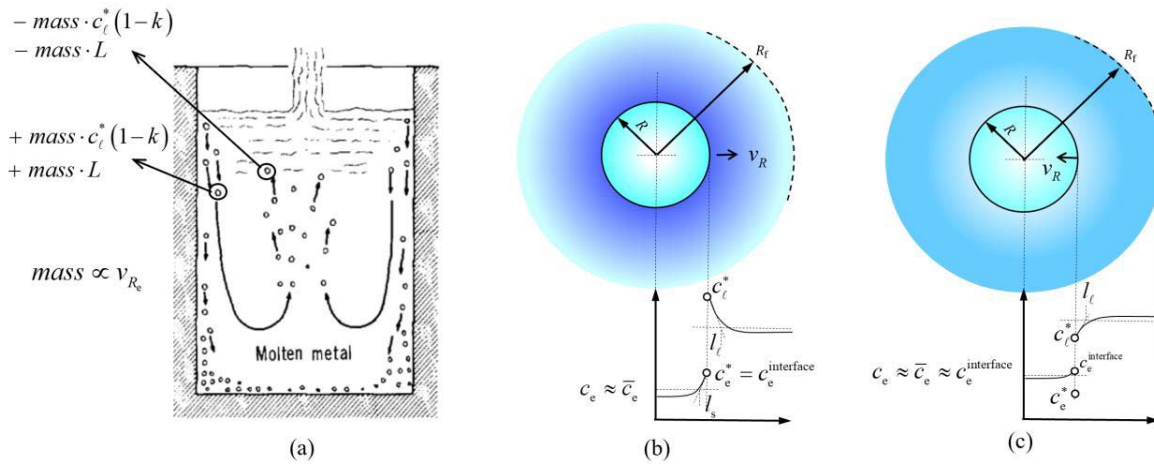
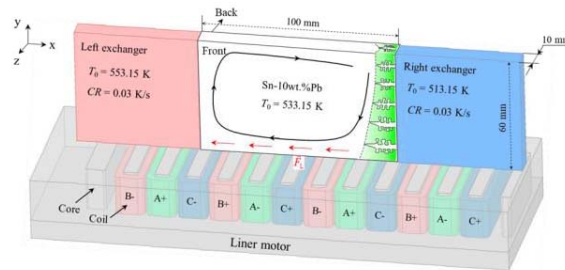


**Figure 1.** Schematics of (a) solidification, grain motion and remelting during solidification of an ingot casting; schematic of the diffusion-governed growth (b) and remelting (c) of a globular crystal. The flow affects the diffusion length  $l_\ell$  during solidification/remelting.

**Figure 2.** Geometry configuration of the experiment facility of the solidification benchmark with TMF [6].



## 2. Methods

A three-phase mixed columnar-equiaxed solidification model [4, 5] is used to study a solidification benchmark ( $100 \times 60 \times 10 \text{ mm}^3$ ) on the Sn-10wt.%Pb alloy as performed at SIMAP laboratory [6]. This conference contribution focuses on the flow-effect on the remelting/solidification of settling/floating globular

equiaxed crystals. Therefore, only details of the corresponding modelling part are described by equations (1) - (3), the rest refers to [4, 5]. Four benchmark experiments at the SIMAP were performed [6]: solidification under natural convection condition, and solidification under forced convections (TMF: travelling magnetic field) with the Lorentz force acting in different directions. As shown in figure 2, only one experiment with TMF acting in the direction from-right-to-left in the bottom of the benchmark is considered in the current study. Two heat exchangers were applied to control the heating/cooling rate on both lateral walls of the sample. The solidified sample was metallographically analysed for the as-cast structure and macrosegregation. Settings for the numerical model, including boundary and initial conditions, material properties, were presented elsewhere [7, 8]. 3 cases are simulated: Case A considers all solidification/remelting and flow effect; Case B ignores the remelting; Case C considers the remelting, but it ignores the flow-effect.

### 3. Results

#### 3.1. Numerical reproduction of the experimental benchmark

Case A represents the most complete scenario. Its solidification sequence (time = 180, 420, 1020, 1920 s) is shown in figure 3. As the benchmark is cooled from right side, solidification starts with columnar structure from right wall, as seen in figure 3 (a.1) - (f.1) at 180 s. The applied TMF (Lorentz force) acts in the same direction as the thermo-solutal buoyancy; hence a strong clockwise convection loop form. The cooler melt from the right side is brought along the sample bottom towards the hotter left side. Equiaxed crystals form by the mechanism of crystal fragmentation [7] in the front of columnar mushy zone. The volume averaged solidification rate is very high ( $M_{\ell c} \sim 80 \text{ kg/m}^3/\text{s}$ ) just ahead of the columnar tip front. The equiaxed crystals are also brought by the melt flow to the hotter region (bottom), where remelting ( $M_{\ell c} \sim -50$ , even reaches  $-80 \text{ kg/m}^3/\text{s}$ ) occurs. It means that during the initial stage of the solidification (180 s), equiaxed grains, which form in the cold region, are almost re-melted in the hotter region. To a later moment (figure 3 (a.2) - (f.2) at 420 s), the same phenomena continue. Some equiaxed grains are brought to the left side of the sample and remelt there. The columnar tip front starts to tilt, and channel segregates start to form in the lower part of the columnar mushy zone. At 1020 s (figure 3 (a.3) - (f.3)), the superheat region disappears. Fragmentation and solidification of equiaxed grains continue with less intensity, but no remelting occurs. Finally, most equiaxed grains are brought to the left side of the sample, and the right side is occupied by columnar structure. Relatively strong channel segregates in the lower-right region of the sample. Globally, relative strong negative segregation occurs in the upper region; very strong positive segregation occurs in the lower left region.

The final as-cast structure and macrosegregation pattern are shown in figure 4, and compared with the experimental results. Excellent qualitative agreement was obtained. The as-cast structure of the experiment cannot be quantified. Quantitative result of macrosegregation shows that the negative segregation in the upper wall and the positive segregation in the bottom wall seem to be overestimated by the model.

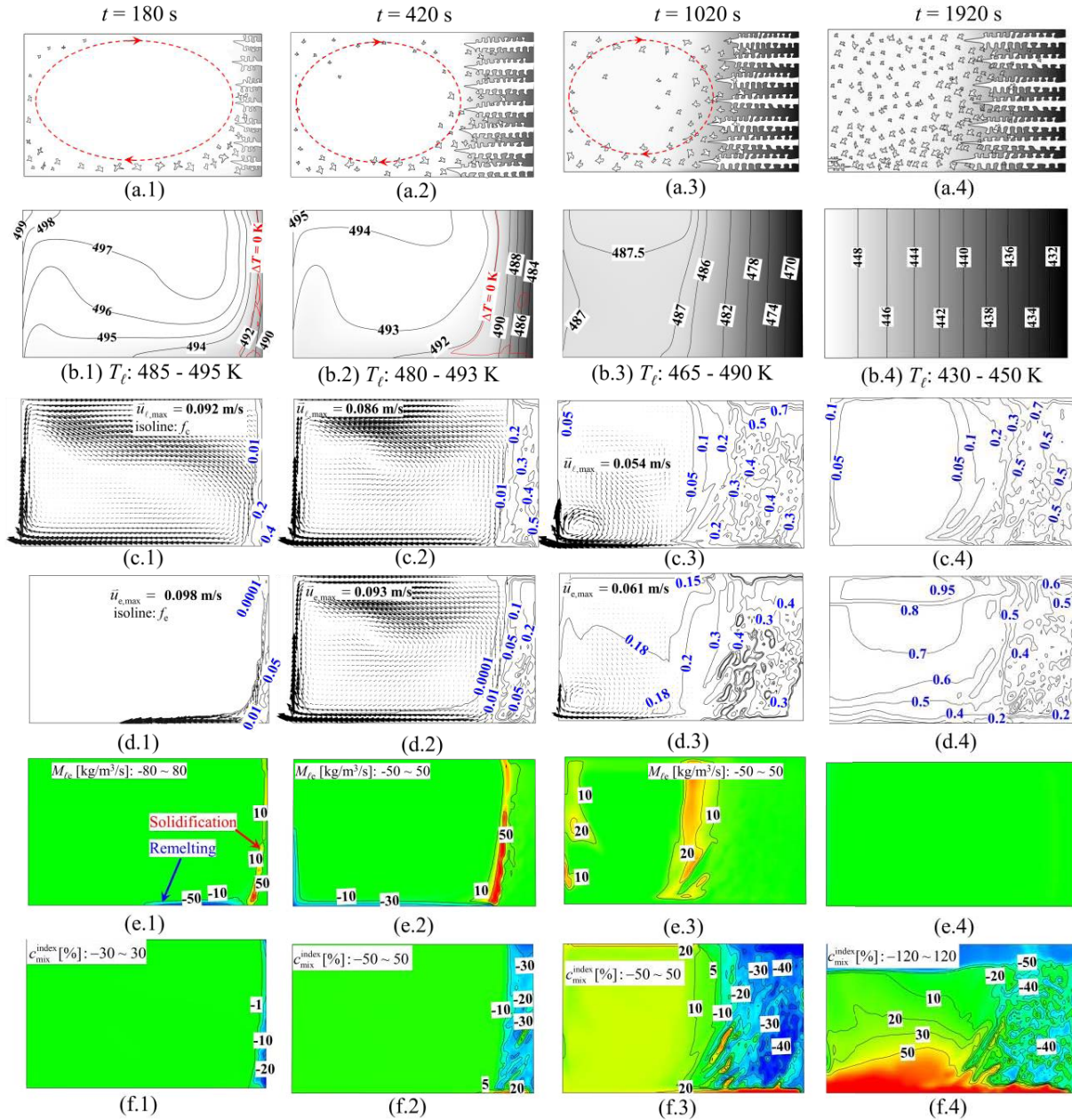


**Figure 3.** Solidification sequence (on the middle vertical plane) of the benchmark (Case A): (a.x) schematic views of the liquid flow and solidification pattern; (b.x) contour and isolines (in black) of  $T$  (in K) overlaid with the red iseline of liquidus (identical to the undercooling  $\Delta T = 0$  K); (c.x) liquid velocity overlaid with the isolines of  $f_c$ ; (d.x) velocity of equiaxed grains overlaid with the isolines of  $f_c$ ; (e.x) contours of  $M_{le}$ , yellow/red regions for solidification ( $M_{le} > 0.0$ ) and blue regions for remelting ( $M_{le} < 0.0$ ); (f.x) contours of the  $c_{mix}^{index}$  [%], yellow/red regions for the positive segregation ( $c_{mix}^{index} > 0.0$ ) and blue regions for negative segregation ( $c_{mix}^{index} < 0.0$ ).



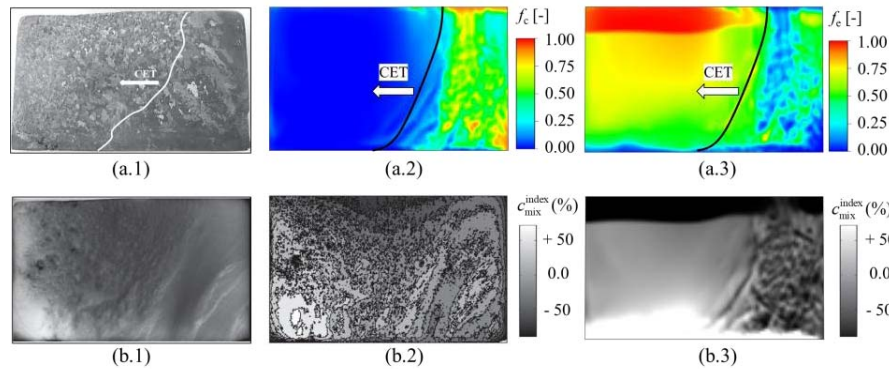


**Figure 4.** Comparison of the simulation result (Case A) with the experiment. (a.1) as-cast structure of the experiment; (a.2) simulated  $f_e$  distribution; (a.3) simulated  $f_e$  distribution; (b.1) X-radiography of the as-cast sample, which indicates the intensity of macrosegregation through the sample thickness; (b.2) macrosegregation map digitally processed from (b.1); (b.3) simulation result of  $c_{\text{mix}}^{\text{index}}$  through the sample thickness.

### 3.2. Importance of the remelting phenomenon

Case B has ignored the remelting of equiaxed phase, i.e. equiaxed grains which are brought to the left side do not re-melt despite of the superheat. Its modelling result for the moment at 420 s is shown figure 5, and compared with that of Case A (complete scenario with remelting). Differences between two cases are observed. (1) The average temperature in the sample of Case B is ca. 1 ~ 2 K higher than that of Case A. Remelting of equiaxed crystals in the left-side superheat region in Case A consumes energy (latent heat), leading to a lower-down of the local temperature. This effect will further influence the temperature field in the rest domain due to convective heat transfer. It means that the ignorance of the remelting phenomenon in Case B has overestimated the temperature in the sample. (2) the remelting of equiaxed crystals does not only influence the solidification of equiaxed phase itself, but it also influences the solidification of columnar structure from the right side. The solidification of columnar structure is also slowed-down by the ignorance of the remelting of equiaxed phase in Case B. This effect is indirect, because Case B has overestimated the temperature everywhere and the growth of columnar structure becomes slower. (3) The velocity is also different, i.e. the maximum velocities (appear at the bottom left corner) of the melt and the equiaxed phase are underestimated in Case B. This might be due to the accumulation of the equiaxed grains (due to the ignorance of the remelting function) in the bottom left corner, which resists the flow in Case B. (4) The remelting-induced dilution of solute in the superheat region is ignored in Case B. This result is not presented in this paper due to limited space. (5) Another interesting phenomenon is also observed: the ignorance of remelting of equiaxed crystals in Case B does not necessarily mean more equiaxed structure to form. It is true that the as-created equiaxed crystals in Case B would survive forever (as the remelting function is completely 'switched-off'), even they are shortly exposed in a superheat region. However, the higher temperature in Case B would suppress the formation of growth of both columnar and equiaxed structures. The final as-cast structure shows that the total equiaxed amount is overestimated only by ca. 13% in Case B. (6) More equiaxed phase is found in the columnar-dominant region along the right-wall region in Case B. Those equiaxed phase comes from the equiaxed crystals, which survive the superheat (due to the ignorance the remelting function) and finally are brought back and entrapped in the columnar structure along the upper part of the right-side wall. This phenomenon occurs in the early stage of solidification. However, it does not happen to Case A. Almost all equiaxed crystals created during the early stage of solidification are mostly (almost all) re-melted by the superheat, and no (almost no) equiaxed crystals can survive the superheat and be brought back in the columnar structure along the right-side wall.

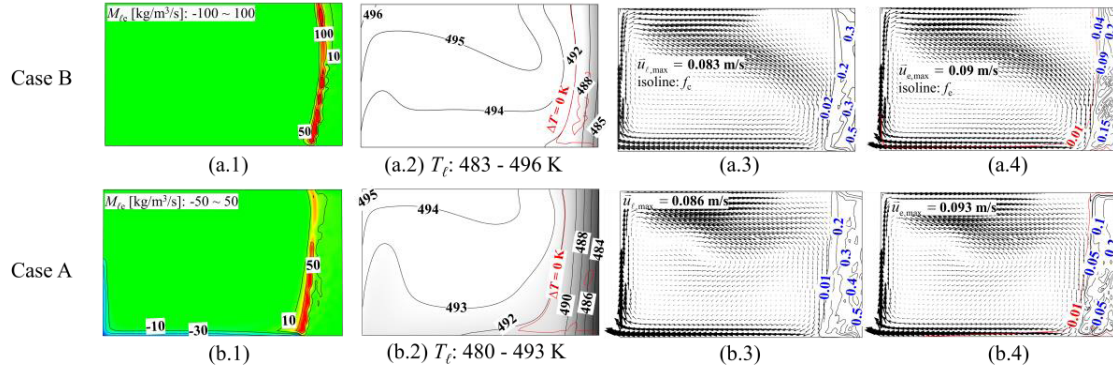


**Figure 5.** Importance of remelting phenomenon: comparison of Case B with Case A for the moment at 420 s. (x.1) contours of  $M_{\ell e}$ , yellow/red regions for solidification ( $M_{\ell e} > 0.0$ ) and blue regions for remelting ( $M_{\ell e} < 0.0$ ); (x.2) contour and isolines (in black) of  $T$  (in K) overlaid with the red isoline of liquidus (identical to the undercooling  $\Delta T = 0$  K); (x.3) liquid velocity overlaid with the isolines of  $f_c$ ; (x.4) velocity of equiaxed grains overlaid with the isolines of  $f_c$ .

### 3.3. Flow-effect on the remelting

Case C has considered the remelting of equiaxed grains, but the flow-effect is not treated properly. The diffusion length (equation (3)) is simply set as the radius of the grain ( $R$ ), i.e. the Reynolds number ( $Re$ ) is set zero. As shown in figure 6, the comparisons of the as-cast structure between the three cases are made. The difference between Case A and Case B is significant. The calculated as-cast structure of Case C is closer to the Case A than to Case B, e.g. the final amount of equiaxed phase of Case C is only about 0.04% over-estimated in comparison to Case A.

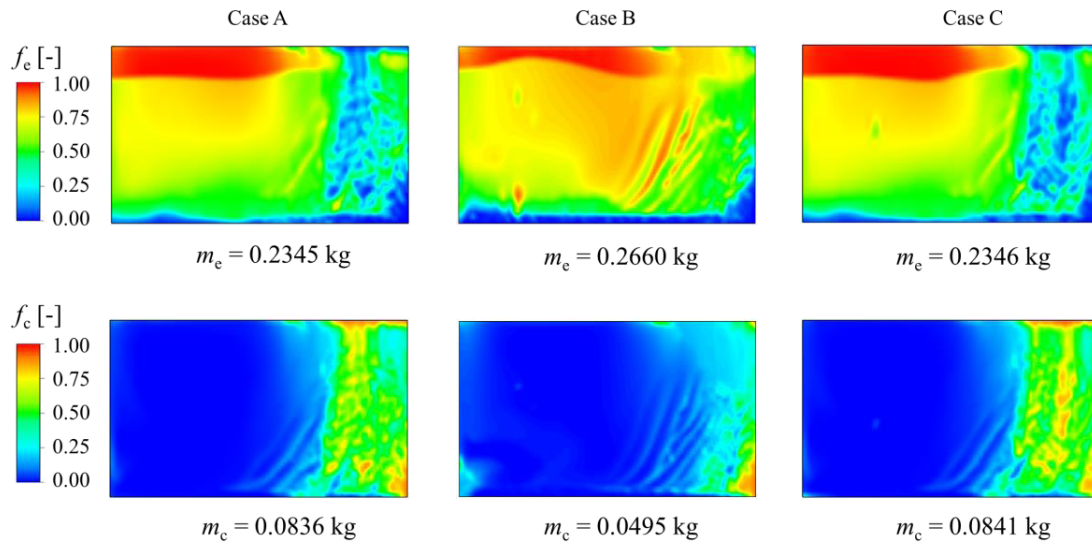


**Figure 6.** Comparisons of the as-cast structure between the three cases.

To further investigate the flow-effect on remelting phenomenon, some relevant solidification parameters at the bottom-left corner of the sample at the moment of 320 s (where/when remelting is significant) are analysed for the Case A. The relative velocity,  $|\Delta u| = |\vec{u}_l - \vec{u}_e|$ , is 0.2 mm/s; the averaged grain side  $d_e (= 2R)$  is 50.0  $\mu\text{m}$ ; the  $Re$  is 0.09; according to equations (3) and (1), the calculated diffusion length  $l_d$  and shrinkage

(remelting) velocity  $v_R$  are  $18.0 \mu\text{m}$  and  $-20.0 \mu\text{m/s}$ , correspondingly. If we ignored the flow-effect by imposing  $Re$  to zero, the calculated  $l_e$  would be  $25.0 \mu\text{m}$  (38.9% overestimation) and  $v_R$  would be  $-17.0 \mu\text{m/s}$  (15.0 % underestimation). The 15.0 % underestimation of  $v_R$  means ca. 38.6 % underestimation of mass remelting rate. In other words, the mass remelting rate as estimated by ignoring the flow-effect is only about 3/5 of what it should be.

#### 4. Conclusion and discussions

To explain the as-cast structure and macrosegregation in the solidification benchmark at SIMAP laboratory [6], one needs to understand the origin of equiaxed crystals by crystal fragmentation, growth, transport and remelting of the equiaxed crystals. As a unidirectional heat transfer condition (cooling from right-side and heating from left-side) and forced convection (TMF) are imposed to the solidification sample, the equiaxed crystals as-formed from the cooler side can be brought to the hotter side, where it is initially superheated, and remelting of the equiaxed crystals occurs. This conference contribution has demonstrated the importance of such remelting phenomena and forced flow effect. A numerical model ignoring the remelting of the floating/settling crystals would lead to following consequences: overestimation of the temperature, delayed growth of columnar structure, overestimation of the amount of equiaxed, underestimation of flow intensity, error estimation of the macrosegregation and structure distribution. The forced flow interacts with the floating/settling equiaxed grains, and it can enhance the remelting rate by 1.7 times in the bottom-left corner region at a certain moment (might be even more in other regions or moments). It is anticipated that such concurrent phenomena of solidification-migration-remelting of equiaxed crystals should occur in engineering processes such as continuous, semi-continuous castings, ingot and shape castings. To what extent do these phenomena impact the as-cast structure formation in the above engineering processes? Further study is demanded. It might depend on the size of the casting when it is solidified under natural convection condition, or depends on the flow intensity when special flow control measures are implemented such as using electromagnetic stirring etc. A numerical model targeting the as-cast structure and macrosegregation must treat those phenomena properly.

#### 5. Acknowledgements

The authors acknowledge the financial support from the Austrian Research Promotion Agency (FFG) through the project Bridge I (No. 868070) and the Austrian Science Fund in the framework of the FWF-NKFIN joint project (FWF, I 4278-N36).

#### References

- [1] Campbell J 1991 *Castings* (London: Butterworth-Heinemann Ltd)
- [2] Rowe P N and Claxton K T 1965 *Trans. Instn. Chem. Engrs.* **43** T321-T331
- [3] Gu J P, Beckermann C and Giamei A F 1997 *Metall. Mater. Trans.* **28A** 1533-1542
- [4] Wu M and Ludwig A 2006 *Metall. Mater. Trans.* **A 37A** 1613-1631
- [5] Wu M, Ludwig A and Kharicha A 2019 *Metals* **9** 229
- [6] Hachani L, Zaidat K and Fautrelle Y 2015 *Int. J. Heat Mass Transf.* **85** 438-454
- [7] Zhang Z, Wu M, Zhang H, Ludwig A and Kharicha A 2023 *Int. J. Heat Mass Transf.* **208**, 124050.
- [8] Zheng Y., Wu M., Karimi-Sibaki E., Kharicha A and Ludwig A 2018 *Int. J. Heat Mass Transf.* **122** 939-953.